Comments on Inorganic Chemistry
Publication details, including instructions for authors and subscription information:
http://www.informaworld.com/smpp/title~content=t713455155

Materials Synthesis Via Solid-State Metathesis Reactions

Randolph E. Treece; Edward G. Gillan[a]; Richard B. Kaner[a]
[a] Department of Chemistry and Biochemistry and Solid State Science Center, University of California, Los Angeles, Los Angeles, California

To cite this Article Treece, Randolph E. , Gillan, Edward G. and Kaner, Richard B.(1995) 'Materials Synthesis Via Solid-State Metathesis Reactions', Comments on Inorganic Chemistry, 16: 6, 313 — 337
To link to this Article: DOI: 10.1080/02603599508035775
URL: http://dx.doi.org/10.1080/02603599508035775

Materials Synthesis Via Solid-State Metathesis Reactions

RANDOLPH E. TREECE,* EDWARD G. GILLAN and RICHARD B. KANER

Department of Chemistry and Biochemistry and Solid State Science Center, University of California, Los Angeles, Los Angeles, California 90024-1569

Received May 20, 1994

The synthesis of solid-state materials generally requires high temperatures and long reaction times in order to overcome diffusion barriers and achieve homogeneous products. Recently chemical routes using reactive precursors have allowed for greater control over product characteristics including stoichiometry and crystallite size. Here we report on one such method which couples reactive solid metal halides with alkali metal–main group compounds in very rapid, exothermic reactions leading to crystalline products and alkali halide salt byproducts. These solid-state metathesis (SSM) reactions provide synthetic control over product crystallinity, homogeneity, and phase. Important compounds as diverse as metal oxides, phosphides, sulfides, nitrides, and silicides have been synthesized using SSM synthesis. Through extensive examples, this review describes the synthetic versatility of this approach, including routes to homogeneous mixed nonmetal solid solutions, product crystallite size reduction through the addition of an inert heat sink (e.g., NaCl), and the synthesis of metastable high temperature phases. The initiation and propagation of these rapid reactions depends strongly on the chemical properties and reactivity of the precursors. Initiation generally occurs when one precursor changes phase or decomposes, allowing for increased surface contact and more reaction. Once an SSM reaction is

*Current address: Naval Research Laboratory, Code 6674, Washington, D.C. 20375-5345.

Comments Inorg. Chem.
1995, Vol. 16, No. 6, pp. 313–337
Reprints available directly from the publisher
Photocopying permitted by license only

initiated it becomes rapidly self-sustaining and can reach high temperatures (> 1000°C) for very short periods (<2 sec). The results from different systems provide indirect evidence for mechanisms involving either ionic or elemental intermediates in these reactions.

Key Words: *solid-state metathesis, exothermic precursor reactions, materials synthesis, combustion, metal halides*

INTRODUCTION

Traditionally, solid-state chemistry has been concerned with *controlling* the reactivity of solids. The two main categories of solid-state processes are (a) solid–*gas* and (b) solid–*solid* reactions. Solid–gas reactions result in the formation of a product layer which can severely retard the rate of the reaction by acting as a diffusion barrier. A useful example of this is the oxidation of aluminum in air ($2Al + 3/2\ O_2 \rightarrow Al_2O_3$). The Al_2O_3 product layer becomes a protective barrier to the diffusion of both the reactive gas (O_2) into the solid and aluminum out from the solid.[1]

In an analogous manner, solid–solid reactions are also diffusion limited. Traditional synthetic approaches to solid-state chemistry utilize high temperatures for long durations to overcome diffusion limitations. These high-temperature methods are energy intensive and usually result in polycrystalline powders of the thermodynamically stable phase. Recently a considerable amount of effort has been applied to develop synthetic methods which require less energy and allow for greater control over product crystallinity (from amorphous to highly ordered), homogeneity, and phase (including metastable structures).[2]

The interest in overcoming diffusion barriers and increasing the reactivity of solids has led investigators to focus on improving mixing and decreasing the particle sizes of the reactants in both elemental and precursor syntheses. One elemental process, discovered by Soviet researchers over 25 years ago, takes advantage of the increased reactivity of small particles to form thermodynamically stable products.[3] They found that an intimate mixture of two finely powdered elements could be ignited with a heated coil or laser pulse and results in an exothermic, self-propagating reaction, later termed self-propagating high-temperature synthesis (SHS). This reaction route

is capable of producing many important materials including borides, carbides, nitrides, oxides, and intermetallics.[4]

While SHS reactions can usually be ignited with little energy input, they still lack effective control over product crystallinity and phase, with incomplete reactions leaving elements in the product. Precursor methods, on the other hand, have provided some degree of product control. By utilizing molecular-scale mixing, homogeneous and stoichiometric binary metal oxides have been synthesized from the precipitation and low-temperature thermolysis of single-source precursors (e.g., $Ba[TiO(C_2O_4)_2] \rightarrow BaTiO_3$).[5] Another promising low-temperature precursor method to oxide ceramics is the sol-gel process which involves conversion of a concentrated solution of hydrolyzed metal alkoxides (sol) into a semirigid metal oxide gel upon removal of the solvent.[6] The sol-gel and aqueous precipitation techniques have been used to control the formation of noncrystalline solids and to synthesize complex oxides.[7] Recent precursor routes to non-oxide materials include the decomposition of inorganic or organometallic precursors to form borides,[8] nitrides[9] and phosphides[10] and the use of pre-ceramic polymers[11] to produce refractory ceramics. In all of the above cases, high temperature annealing is required to produce crystalline compounds.

SOLID-STATE METATHESIS (SSM) REACTIONS

Our research has focused on developing a new, general solid-state precursor route to materials. This method involves rapid, low-temperature initiated solid-state metathesis (SSM) reactions between two intimately mixed solid precursors which can be ignited with a hot filament. There are a few early examples of related solid-state metathesis (exchange) reactions involving heating precursors, although this method was never pursued to any great extent.[12] As it turns out, a very broad range of materials can now be prepared in seconds from self-propagating SSM reactions.[13] A generalized reaction scheme is shown below:

$$MX_m + m\,AY_n \xrightarrow{\text{ignite}} MY_z + m\,AX + [(m \cdot n) - z]Y \qquad (1)$$

where M represents a metal, X a halide, A an alkali metal, and Y a nonmetal or metalloid. In a helium-filled dry box, the precursors are mixed together, loaded into a reaction vessel modeled after a Parr bomb calorimeter,[14] and ignited by brief (<2 sec), local heating from a hot filament. The alkali halide byproduct is removed by simply washing with methanol and/or water, leaving the polycrystalline products. The driving force in all of these reactions is the formation of very stable alkali halide salts. These self-sustaining reactions are designed to be highly exothermic, generating a great deal of heat which lasts only seconds. Materials produced by this method include nitride superconductors (e.g., NbN and ZrN),[13,15] 13–15 semiconductors (e.g., GaAs and InSb),[16,17] insulating ceramics (e.g., BN and ZrO_2),[18,19] magnetic materials (e.g., GdP and SmAs),[20] transition-metal pnictides (e.g., ZrP and NbAs),[21] oxides (e.g., Cr_2O_3 and CuO),[19] chalcogenides (e.g., MoS_2 and NiS_2),[22] and refractory intermetallics (e.g., $MoSi_2$ and WSi_2).[23] Along with the binary materials, mixed–metal (e.g., $Mo_xW_{1-x}S_2$ and $Al_xGa_{1-x}As$)[24] and mixed-nonmetal (e.g., $MoS_{2-x}Se_x$ and GaP_xAs_{1-x})[18b,25] ternary compounds can also be prepared from the appropriate solid-solution precursors. This article outlines the general approach and wide applicability of SSM synthesis, demonstrates how this process allows for significant control over product crystallinity, homogeneity, and phase, and then concludes with a discussion of proposed mechanistic pathways.

SYNTHETIC CONTROL

Self-sustaining SSM reactions have several advantages over traditional high-temperature syntheses. One advantage is the rapid synthesis of high-quality materials in which one of the elements has a high vapor pressure at elevated temperatures, e.g., oxides, nitrides, arsenides, and phosphides. As an example, important ceramic nitrides such as TiN and BN have been prepared via SSM routes using the solid precursor nitrogen sources, Li_3N and NaN_3. Whereas the industrial production of hexagonal boron nitride (h-BN) involves high temperature (> 1500°C) reactions between boron oxide and ammonia,[26] highly crystalline h-BN can be prepared in seconds by a rapid SSM reaction between $NaBF_4$ and Li_3N initiated by a hot filament.[18a] In addition, transition metal nitrides with interesting elec-

tronic properties can be synthesized using similar reactions.[15b] For example, zirconium nitride (ZrN), a superconductor with $T_c \approx 10$ K, is typically prepared under high temperatures and nitrogen pressures,[27] but SSM methods have been used to produce the cubic, superconducting ZrN (see Fig. 1) in seconds using the following precursor mixture:

$$ZrCl_4 + 4/3\ Li_3N \rightarrow ZrN + 4LiCl + 1/6\ N_2. \qquad (2)$$

Further evidence of the utility of this approach in overcoming problems associated with traditional synthetic methods is in the rapid preparation of refractory intermetallics, such as WSi_2 (mp = 2150°C). WSi_2, due to the refractory nature of W and Si, is very difficult to prepare by traditional high-temperature methods; however, it can be rapidly synthesized from WCl_6 and Mg_2Si as shown below[23]:

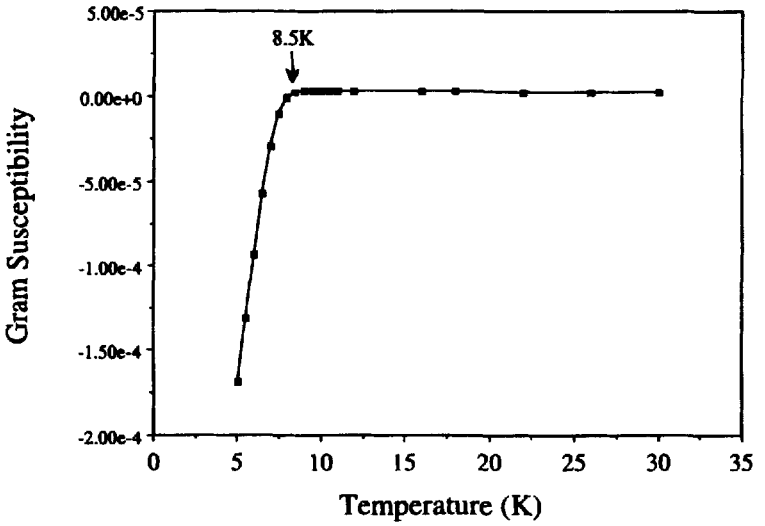

FIGURE 1 Plot of magnetic susceptibility versus temperature for ZrN synthesized in seconds from $ZrCl_4$ + 4/3 Li_3N. The arrow shows the onset of diamagnetic shielding indicative of superconductivity.

$$WCl_6 + 3/2\ Mg_2Si \rightarrow 3/4\ WSi_2 + 3\ MgCl_2 + 1/4\ W. \quad (3)$$

If desired, the tungsten byproduct can be removed by washing with aqua regia.

INITIATION AND PROPAGATION

The ignition process is an important consideration in SSM synthesis. While many of the metathesis reactions self-initiate, others require some thermal input, coming from sources such as frictional heating (e.g., grinding in a mortar and pestle), a hot filament (e.g., nichrome wire with $T \leq 850°C$), or a laser pulse. Phase transitions and decomposition points of the precursors are the major factors influencing the initiation conditions. Since vaporization, melting, and/or decomposition of at least one of the precursors increases surface contact, such a structural change with generally initiate a self-propagating reaction. The propagation of the reaction requires that the heat generated in the initial steps is sufficient to cause further reaction to proceed unassisted throughout the bulk. Thus the exothermicity of the overall reaction generally determines to what extent propagation occurs.

The strong link between a compound's melting and boiling points and its structure allow investigations of the relationship between structure and initiation conditions. Such a relationship is illustrated by the formation of 13–15 (formerly called III–V) semiconductors in the following series of reactions:

$$GaX_3 + Na_3P \rightarrow GaP + 3\ NaX \quad (4)$$

where X represents the halides I^-, Cl^-, or F^-. Melting and/or vaporization of the gallium halide precursor appears to be the initial step in the reactions involving GaI_3 and $GaCl_3$.[17] A breakdown of these precursors is followed by production of the sodium halide byproduct, with subsequent formation of GaP occurring within a molten reaction flux. GaI_3 is a molecular crystal with low melting (212°C) and sublimation (345°C) temperatures, and reactions with this precursor can be initiated by light grinding with a mortar and pestle. Isostructural $GaCl_3$ melts at 78°C and reactions with it self-initiate within seconds

after mixing the precursors. Reactions with GaF_3, however, do not self-initiate. GaF_3 adopts a three-dimensional network structure and sublimes at temperatures greater than 800°C. It appears that a phase change in the pnictiding agent (i.e., Na_3P decomposition at >550°C) is needed to initiate the reaction between GaF_3 and sodium phosphide. The absence of self-initiating reactions between the fluoride and pnictide precursors can be explained by the lack of any appreciable vapor pressure from either precursor at room temperature. When neither precursor decomposes or melts significantly below temperatures achieved by the hot filament (~ 850°C), a self-sustaining reaction generally cannot be initiated by this method. The formation of GdN is an example where both of the precursors melt/decompose at temperatures above ca. 800°C. In this case, the reaction between GdI_3 (mp = 930°C) a three-dimensional network solid and Li_3N (mp = 813°C), cannot be initiated with a hot wire. A summary of these precursors' properties[28] and their initiation conditions is given in Table I.

Next it is beneficial to examine the steps immediately following the melting of metal iodide in the presence of Na_3Y (Y = P, As). The breakdown of the MI_3 lattice is followed by a rapid metathesis reaction which results in metal pnictide products, along with the formation of three moles of sodium iodide byproduct. The salt formation accounts for nearly 90% of the reaction enthalpy. The initial surface reaction is expected to play an important role in the self-propagating nature of these reactions, since increasing surface contact by simply grinding the reagents together with a mortar and pestle initiates a reaction in some systems. The extent of initial surface reaction was examined by lightly grinding, but not initiating, a reaction between GaI_3 and Na_3As. A powder X-ray diffraction (XRD)

TABLE I

Melting/decomposition points and initiation conditions

MX_3	mp. (°C)	A_3Y	Decomp. (°C)	Initiation Conditions
$GaCl_3$	78	Na_3P	>550	Stirring Together
GaI_3	212	Na_3P	>550	Grinding w/Mortar & Pestle
GaF_3	800, sub.	Na_3P	>550	Heating w/Hot Wire
GdI_3	930	Li_3N	813	*Not Initiated by Hot Wire*

pattern of the resulting reaction mixture reveals the formation of partially crystalline NaI along with the starting materials (Fig. 2). This shows that although some initial surface reaction has occurred, it has not yet generated sufficient heat to initiate a self-sustaining reaction.

Further illustration of a surface pre-reaction occurring at temperatures below the lowest precursor melting point is shown in Fig. 3. Differential scanning calorimetry (DSC) of the reaction between AlI_3 and Na_3P shows a broad exotherm beginning at 100°C, with ignition of the self-propagating reaction occurring just above 200°C. The exothermic event beginning at 100°C is a likely initial surface reaction between the intimately mixed precursors which occurs below the melting point of AlI_3 (mp = 191°C). As the temperature nears the melting point of AlI_3, a large exothermic event occurs, indicating a self-propagating reaction has taken place. Note that there is no appar-

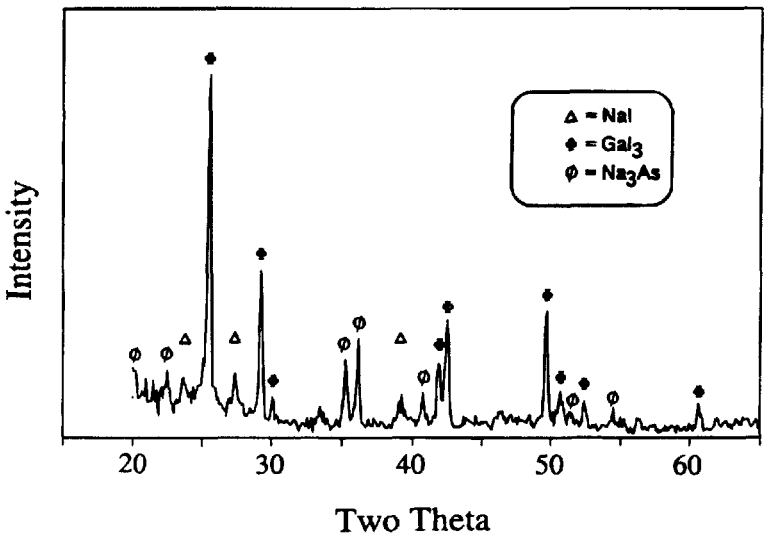

FIGURE 2 XRD pattern of a reaction mixture of GaI_3 + Na_3As after grinding with a mortar and pestle. The precursors were not ignited and therefore are still detectable in the pattern, but surface reaction has already begun as indicated by the appearance of NaI.

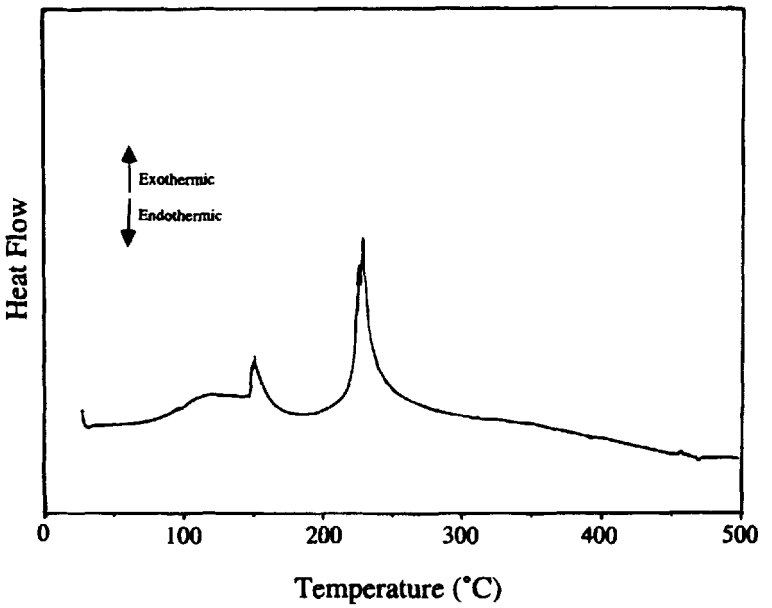

FIGURE 3 A differential scanning calorimetry (DSC) trace of the reaction between AlI_3 and Na_3P. The mixture was heated at 10°C/min in flowing argon.

ent endothermic event due to the melting of aluminum iodide as this is overwhelmed by the immediate exothermic reaction.

Once initiated, these ignited precursor reactions are very exothermic and quite rapid. For example, the preparation of MoS_2 by the following route:

$$MoCl_5 + 5/2\ Na_2S \rightarrow MoS_2 + 5\ NaCl + 1/2\ S \qquad (5)$$

has a calculated enthalpy of reaction (ΔH_{rxn}) based on Hess's law of -213 kcal/mol.[29] Bomb calorimetry results agree well with this theoretical value.[22a] One can compare this ΔH_{rxn} to the well-known thermite reaction ($Al + 1/2\ Fe_2O_3 \rightarrow Fe + 1/2\ Al_2O_3$) where the calculated reaction enthalpy is -102 kcal/mol. The major driving force in Eq. (5) and other SSM reactions is the formation of the very stable salt byproduct (e.g., $\Delta H_f(NaCl) = -98$ kcal/mol).

While most systems can be initiated by a hot filament, not all combinations of a metal halide and an alkali main-group compound are self-propagating. A simple example given by Eq. (6) is the reaction between calcium chloride and a sodium chalcogenide[24b]:

$$CaCl_2 + Na_2X \rightarrow CaX + 2\ NaCl \qquad (6)$$

where X is S, Se, or $S_{0.46}Se_{0.54}$. In this case, a self-propagating reaction could not be initiated with a hot nichrome filament (~850°C), but a product did form around the wire. In order to understand why these reactions do not self-propagate, it is necessary to consider the reaction thermodynamics. The ΔH_{rxn} of Eq. (6) calculated for the formation of CaS is only −34 kcal/mol. Compared to reactions which easily self-propagate, such as $GaI_3 + Na_3As \rightarrow GaAs + 3\ NaI$ (ΔH_{rxn} = −117 kcal/mol), the enthalpy of reaction calculated for the formation of CaS is rather small, due largely to two factors: (1) there are only two moles of salt byproduct per mole of CaS; and (2) the ΔH_f of $CaCl_2$ is relatively high at −190 kcal/mol compared to $\Delta H_f(GaI_3)$ = −57 kcal/mol. Calcium chloride adopts a 3-D framework based on a distorted rutile structure[30] and melts at 782°C. In this case, the heat released by the initial reaction next to the wire is not sufficient to overcome the high melting points of the remaining precursors, $CaCl_2$ and Na_2S (mp = 1180°C). This lack of propagation has been observed with other reaction mixtures when the ΔH_{rxn} was only slightly exothermic (or endothermic) and the precursors have high melting points.[19a]

REACTION TEMPERATURE EFFECTS

Crystallite Size

Currently there is considerable interest in developing techniques which make it possible to produce small particles, such as nanocrystalline semiconductor particles which have interesting optoelectronic properties,[31] and sub-micron sized ceramics which may allow for easier densification and improved physical characteristics.[32] The chemical variability available in SSM reactions allows for some degree of crystallite size control through manipulation of reaction

temperatures and molten salt fluxes generated during synthesis. The rapid release of energy in ignited SSM reactions creates high temperatures which are sufficient to melt or vaporize the reactants and salt byproduct, resulting in the formation of a molten reaction flux which aids in reducing solid-state barriers by increasing diffusion. The maximum temperature achieved by a reaction and the length of time spent at that temperature strongly affects the crystallinity of the products. By controlling the conditions of the reaction flux, it is possible to influence the maximum temperature and duration of a reaction, thereby manipulating the crystallinity of the product. For example, experiments have shown that larger reaction mixtures lead to higher product yields and increased product crystallinity.[15b,17,18a] There is apparently a less significant heat loss to the surroundings because the larger scale reactions provide a better insulated and more homogeneous molten flux. Due to improved insulation, the core of the reaction flux remains at higher temperatures for longer durations than is possible with smaller mixtures. By remaining at elevated temperatures in a molten flux following reaction, the products are more fully crystallized (i.e., self-annealed).[33]

The theoretical maximum reaction temperature (T_{ad}) can be calculated from thermodynamic data[29] assuming no heat is lost to the surroundings in the short timescale of the reaction (an adiabatic system). For example, the T_{ad} for MoS_2 formation given by Eq. (5) is 1413°C, the boiling point of the NaCl byproduct salt as shown in Fig. 4. However, the temperature actually attained can be far less than T_{ad} if there is incomplete reaction or significant heat lost to the surroundings. Using optical pyrometry, it was determined that the MoS_2 reaction reaches temperatures in excess of 1000°C within seconds of initiation and cools to room temperature in less than 30 seconds. More accurate *in situ* measurements with a thermocouple have recorded temperatures for the ZrN reaction (Eq. (2)) that are within a few percent of the theoretical T_{ad} of 1408°C, the boiling point of LiCl.[15b]

Another way to affect self-annealing is to alter T_{ad} through the selection of the appropriate precursors. The relationship between T_{ad} and product crystallinity was investigated using powder XRD and solid-state NMR on GaP materials made from the GaX_3 + Na_3P (X = F, Cl, I) reaction series.[17] Both characterization methods revealed that generally the crystalline quality (crystallite size, defects, and

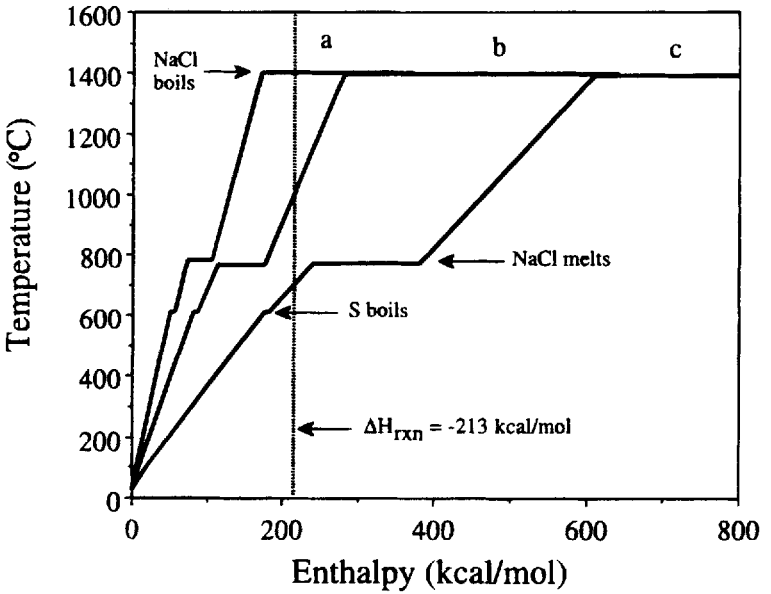

FIGURE 4 Theoretical plots of enthalpy versus temperature for the MoS_2 reaction system with added salt: $MoCl_5$ + 5/2 Na_2S + x NaCl → MoS_2 + (5 + x)NaCl + 1/2 S. The plots are for (a) x = 0, (b) x = 4, (c) and x = 16, where the heat of reaction is used to heat the product mixture to elevated temperatures. The plots are slightly offset at the boiling point of NaCl (1413°C) for clarity.

composition) of the GaP products decreased with decreasing T_{ad}. The reactions with $GaCl_3$ produced a much less crystalline GaP than expected, due to incomplete precursor mixing. Reactions using $GaCl_3$ self-initiate before the precursors can be thoroughly mixed and the heat released melts the unmixed $GaCl_3$, resulting in reaction temperatures substantially lower than T_{ad}. Subsequent reaction between the molten $GaCl_3$ (visible in the mortar) and solid Na_3P likely occurs near $T_{flux} \approx 210$°C.

In addition to providing a reaction medium, the molten salt flux moderates the reaction temperature. In most cases T_{ad} equals the boiling point of the byproduct salt. The addition of an inert heat sink (e.g., NaCl) to the reaction mixture will remove heat normally available for crystallization and also lower the maximum reaction

temperature. For example, the addition of increasing amounts of NaCl to the MoS_2 reaction:

$$MoCl_5 + 5/2\ Na_2S + x\ NaCl \rightarrow MoS_2 + (5 + x)NaCl + 1/2\ S \qquad (7)$$

leads to a systematic decrease in crystallite size.[22a] As x increases from 0 to 16, the crystallite size decreases from 450 Å to 80 Å, showing a reduction in the self-annealing properties of the reaction flux. Calculations of T_{ad} show that there should be a corresponding drop in reaction temperatures from 1413°C to 687°C as reaction enthalpy is used to heat, melt and boil the added NaCl (see Fig. 4). Similar results have been found in other SSM systems.[15b,21a]

Metastable Phases

Besides varying the physical properties of a material, it is also advantageous for precursor routes to have some control over product phase. Considerable research has been applied to the polymorphic ZrO_2 system.[34] In order for zirconia to be a more useful refractory material, stabilizing its high-temperature phase at lower temperatures will be necessary. On heating, ZrO_2 undergoes a monoclinic → tetragonal phase transition at 1100°C and passes from tetragonal → cubic at 2300°C. The lower temperature transition is accompanied by a large volume change which can cause cracking in ceramic parts. While quenching the tetragonal phase to room temperature is very difficult, precipitation and sol-gel routes have resulted in the isolation of poorly crystalline cubic/tetragonal (c/t) ZrO_2.[35] The preparation of crystalline stabilized forms of the c/t-ZrO_2 phase which will not revert to the stable monoclinic form on heating is a current challenge.

Using appropriate solid-state precursors has allowed c/t-ZrO_2 to be synthesized via metathesis reactions. The ignition of a rapid SSM reaction between $ZrCl_4$ and Na_2O results in a mixture of monoclinic and cubic phases.[19a] If, instead, the precursors are gently heated in sealed tubes below their ignition temperature (≈ 300°C), the washed products are amorphous powders (Fig. 5a). Heating this product to 350°C for 12 h leads to the crystallization of metastable c/t-ZrO_2 (Fig. 5b). Further heating of this metastable phase to ~600°C starts

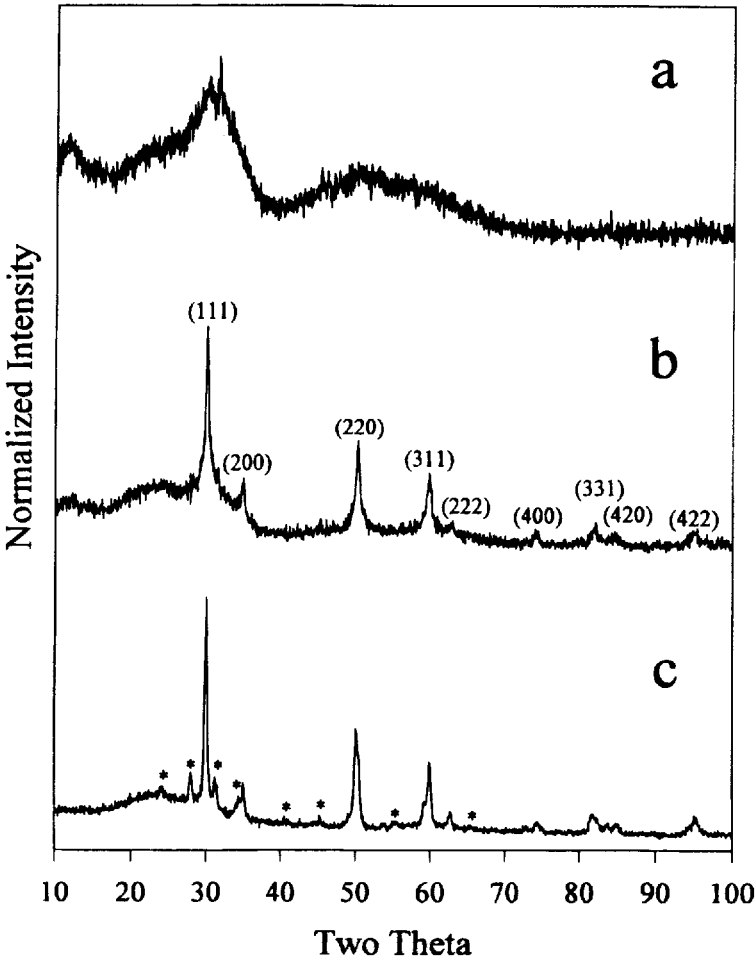

FIGURE 5 Powder X-ray diffraction patterns of the products from the reaction of $ZrCl_4$ and Na_2O (a) heated at 220°C for 5 days and washed, (b) washed product from (a) heated at 350°C for 12 h, and (c) annealed product from (b) heated at 600°C for 12 h. The c/t-ZrO_2 peaks are labeled with (hkl) values and the * indicates the monoclinic phase.

a transformation to monoclinic ZrO_2 (Fig. 5c). The general reaction scheme is

$$ZrCl_4 + 2\ Na_2O \xrightarrow{220°C,\ 5\ days} ZrO_2\ (amorphous) + 4\ NaCl \xrightarrow[(2)\ 350°C,\ 12\ hr]{(1)\ wash} c/t\text{-}ZrO_2. \quad (8)$$

Ongoing research with this metathesis route involves investigating ternary metal substitutions which lead to stabilization of the c/t-ZrO_2 phase to higher temperatures.

The structure of certain refractory alloys also influences physical and mechanical characteristics and often metastable phases exhibit improved properties. For example, because of its high melting point, high conductivity, and resistance to corrosion and oxidation at elevated temperatures, $MoSi_2$ is used as a furnace element. However, its poor ductility is a significant shortcoming to applications of $MoSi_2$ as a high-temperature structural material.[36] Below 1900°C it exists as α-$MoSi_2$ with a tetragonal structure, while above this temperature it is found in the hexagonal β-form. It has been proposed that overall ductility might be greatly increased with an intimate mixture of α and β forms. Crystalline powders with a mixture of α- and β-$MoSi_2$ have been directly synthesized by a rapidly initiated metathesis reaction.[23] This may lead to the possibility of using SSM reactions to form other metastable phases and perhaps even prepare new materials which are not accessible by more traditional approaches.

CONTROL OF TERNARY HOMOGENEITY

Many mixed-metal and mixed-nonmetal solid solutions have been prepared via SSM reactions.[15a,18b,20,24,25] A major difficulty in the formation of ternary solid solutions is achieving nanoscale mixing throughout the material. SSM processes make it possible to achieve homogeneous ternary products because they can utilize atomic scale-mixed solid-solution precursors. An illustrative comparison can be made between the three "ternary" reaction systems shown below:

$$GaI_3 + 1/2\ Na_3P + 1/2\ Na_3As \xrightarrow{\text{ignite}} Ga(P,As) + 3\ NaI \quad (9)$$

$$GaI_3 + Na_3P_{0.5}As_{0.5} \xrightarrow{\text{ignite}} Ga(P,As) + 3\ NaI \quad (10)$$

$$GaI_3 + Na_3P_{0.5}As_{0.5} \xrightarrow{\text{ignite}} \xrightarrow{500°C,\ 12\ hr} Ga(P,As) + 3\ NaI. \quad (11)$$

In the first reaction (Eq. (9)), the binary pnictide precursors were physically mixed by thorough grinding before being stirred together with the gallium iodide and ignited. In the second and third reactions (Eqs. (10) and (11), respectively), a solid-solution precursor was used. The advantage of using a solid-solution precursor is clearly displayed in Fig. 6, which shows the XRD patterns of the three Ga(P,As) products. The diffraction lines of the material resulting from the physical mixture of pnictides (Fig. 6a) are inhomogeneously broadened relative to the products from the solid-solution precursor (Fig. 6b). This type of broadening is indicative of significant compositional gradients and variations in regional stoichiometry. Despite good *physical* mixing of the micron sized powders, the P and As atoms are still very localized within the reaction mixture compared to the homogeneous dispersion possible with atomic-level *chemical* mixing. Figure 6c shows how further heating in addition to that provided by ignition (Eq. (11)) improves the homogeneity and crystallinity of the Ga(P,As) product prepared from the ternary precursor.

POSSIBLE REACTION PATHWAYS IN SSM SYNTHESIS

The discussion of reaction pathways will focus on initiation and propagation of metal–nonmetal and metal–metalloid systems. The proposed steps involved in initiation have been detailed in the Initiation section above. Briefly, ignition occurs when sufficient heat has been provided to the precursor mixture to cause a phase change or

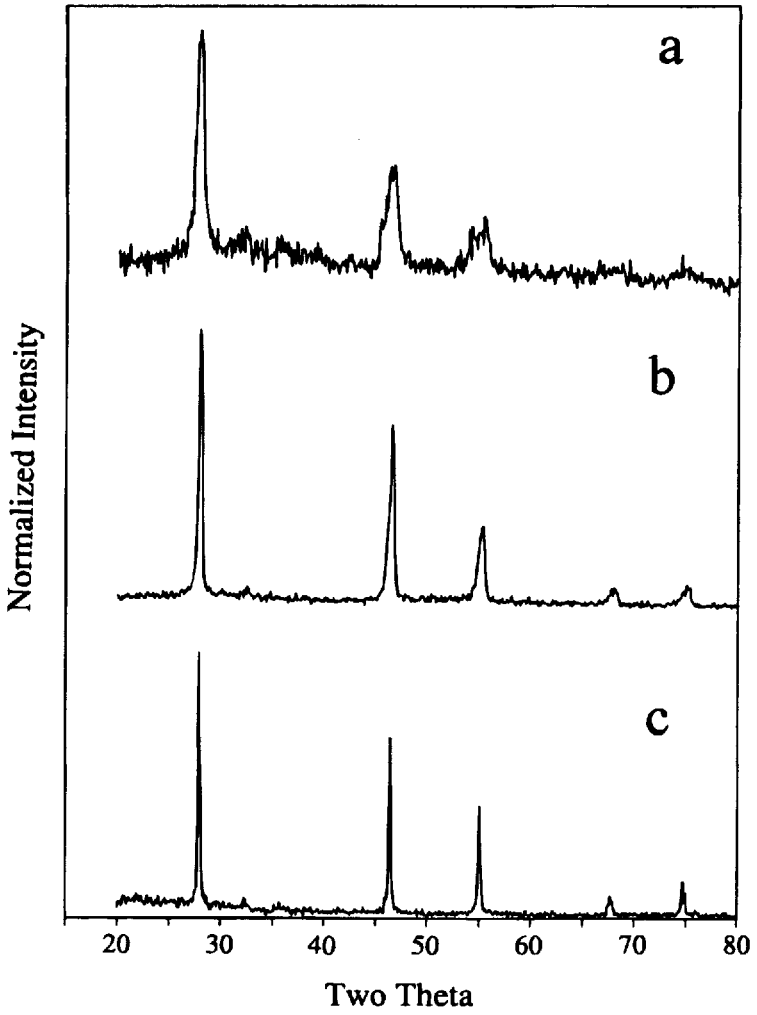

FIGURE 6 Powder X-ray diffraction patterns of Ga(P,As) produced by ignition reactions between GaI_3 and (a) 1/2 Na_3P + 1/2 Na_3As, (b) $Na_3P_{0.5}As_{0.5}$, and (c) $Na_3P_{0.5}As_{0.5}$ followed by heating at 500°C for 12 h.

decomposition in one of the precursors. This is followed by salt formation, since XRD evidence indicates that production of some salt byproduct occurs before the complete loss of either precursor. The initiation process appears relatively straightforward, but discerning the intermediate stages toward product formation is quite challenging. Once ignited, the brief, exothermic nature of these precursor reactions makes it very difficult to directly observe mechanistic steps or intermediate species by traditional solid-state techniques such as X-ray diffraction. Due to this difficulty, speculation about mechanisms requires one to analyze the end products and then to infer the steps which might lead to these materials. Just after ignition of a reaction, under the extreme conditions produced, there are likely to be a variety of chemical species present, such as the byproduct salt, precursor molecular fragments, free elements, and ions in various oxidation states.

Even though the actual reaction pathway is probably quite complicated, the mechanism might simplistically be modeled as a competition between two different processes. These competing models are "elemental" and "ionic" routes. In the elemental route, a redox reaction takes place between the precursors which results in metal (M) and non-metal (Y) elements present in an alkali halide (AX) salt, with subsequent MY product formation within the molten salt flux. The ionic route involves reaction between the M^{3+} and the Y^{3-} ions in the molten AX flux, where thermal energy allows atomic rearrangement through attractive forces. A schematic of these competing pathways is presented below.

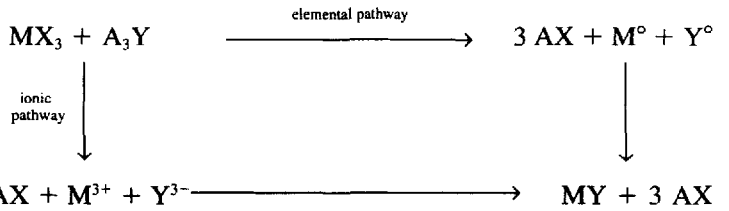

Although neither of these pathways can be observed directly, each does have characteristics which could lead to different observable reaction end products. In the elemental model, the production of MY material will take place only as long as heat is present, but on cooling

the reaction is quenched. This process will be limited by the amount of heat generated, the ease of product formation, and the cooling rate. In the ionic model, the effect of rapid cooling can be expected to prevent self-annealing of the quickly formed products, leading to amorphous materials, but not prevent MY formation. Moving under electrostatic forces, the relatively short distances between the reactive ions would be traversed easily at the high reaction temperatures. There is evidence for both pathways in ignited SSM reactions. The elemental route seems to be taken by the transition metal dichalcogenides and the 13–15 semiconductors. The ionic pathway is observed by the magnetic pnictides and alkaline earth chalcogenides. A brief review of selected results on these systems, including binary and ternary reactions, and how they apply to mechanistic considerations is discussed below.

Binary Reactions

The first system providing evidence for an elemental route is the 13-15 materials. The products of the ignition of InI_3 and Na_3P, along with InP and NaI, include indium metal, reduced indium iodide (InI_2), and red phosphorus.[17] The presence of elemental species and InI_2 suggest that the reaction process involves a redox reaction between In^{3+} and P^{3-} within the flux. In this case, neither the redox nor the subsequent reaction between the elements goes to completion. The oxidizing power of the iodide ligands is not sufficient to prevent reduction of In^{3+} by P^{3-} in the reaction flux. In fact, redox occurs in all of the InI_3 + Na_3Pn (Pn = P, As, or Sb) precursor reactions as evidenced by the presence of elemental indium and/or pnictogen in the products. Sustained heating of the precursors in sealed glass ampoules produced the 13–15 materials without contamination by excess metal, pnictide or reduced metal iodide.

Other supporting examples from the 13–15 materials include GaP and GaAs. Ignited SSM reactions between GaI_3 and Na_3Pn produced XRD pure GaP and GaAs.[16] However, examination by optical and electron microscopy revealed the presence of gallium spheres and red phosphorus clumps in the washed products.[17] When the precursors were heated in glass ampoules to 550°C for 8 h instead of ignited in a reaction bomb, the products did not contain excess free elements.

Additional evidence for an elemental pathway in ignited SSM reactions can be found in the preparation of WTe_2.[25] While the sealed

tube reaction between WCl_6 and Na_2Te produces WTe_2, the ignition process does not. The washed ignition products contain only elemental tungsten and tellurium. It is likely that following initiation of the precursor mixture, a redox reaction between W^{6+} and Te^{2-} occurs, leading to W^0 and Te^0. The subsequent formation of WTe_2 takes place within the NaCl flux. Sustained heating within a sealed tube provides the heat and time necessary for the reaction between W and Te to proceed to its thermodynamic end, the formation of WTe_2. The presence of W and Te in the products of the ignited reactions indicates kinetic quenching of the reaction between the zero-valent elements caused by rapid cooling of the flux.

Considerable evidence for an ionic route can be found in the SSM synthesis of 3–15 materials (e.g., GdP).[20a] The washed products of ignited reactions between GdI_3 + Na_3Pn (Pn = P, As, or Sb) do not contain any excess pnictogen and have less than 0.3 percent free metallic gadolinium as detected by field-dependent magnetic susceptibility. The virtual absence of free elements in the GdPn systems can be contrasted with the metal dichalcogenides and 13–15 compounds described above. The presence of elements in the endproducts of 3–15 reactions would be expected if an elemental pathway were followed, since reactions between gadolinium and phosphorus typically require long periods of time (> 50 h) at elevated temperatures (> 900°C) to go to completion.

More evidence for an ionic pathway can also be inferred from the GdSb system. The ignited SSM reaction produces an XRD amorphous product, in contrast to GdP and GdAs which are microcrystalline. The inverse susceptibility versus temperature curve for the amorphous GdSb sample, however, is qualitatively similar to the curves resulting from the crystalline GdP and GdAs samples. The bulk magnetic susceptibility of GdSb is what is expected for a paramagnetic substance contaminated with traces (< 0.3%) of a ferromagnetic impurity, as was seen for GdP and GdAs. This implies that the vast majority of gadolinium atoms in GdSb are in the form of Gd^{3+} ions, and that they are coordinated to Sb^{3-} ions (as in the crystalline analogs), but there is little long range order. In this case, the reaction cools before the small GdSb particles can grow into large crystalline domains. Crystalline order is not a prerequisite for the observed paramagnetic susceptibility since these characteristics arise from localized Gd^{3+} ions. It is also important that even though

GdSb does not crystallize as well as the GdP and GdAs samples, the amorphous products do not contain any more free Gd metal than measured in GdP or GdAs. Since it is expected that the species quenched in the amorphous state will reflect the reaction intermediates, the absence of substantial amounts of free gadolinium in the amorphous powders is further evidence that the intermediates are not in their elemental (zero valent) states in the molten flux.

Ternary Reactions

In order to achieve a ternary product with a homogeneous distribution of substitutional atoms, it is advantageous to use a well-mixed solid-solution precursor. But even when an atomically mixed precursor is employed, the composition of the product may differ from that of the ternary reagent. It is expected that when metathesis reactions are performed in sealed tubes at high temperatures, the composition of the precursors is conserved in the products; however, when the precursor mixture is ignited, the composition of the precursor may not be conserved in the resulting ternary compound. Whether the stoichiometry of the ternary precursor is conserved in the product provides information about the reaction pathway. We believe that conservation of precursor composition is associated with an ionic route and deviation from stoichiometry is linked to the elemental pathway. So far, two ternary systems have been observed to follow an ionic route: Gd(P,As) and Ca(S,Se), while two others appear to take an elemental pathway: Ga(P,As) and $Mo(S,Se)_2$.

Ignition reactions between GdI_3 and the solid-solution precursors $Na_3P_xAs_{1-x}$ ($x = 0.25$, 0.50 or 0.75) produced the ternary compounds GdP_xAs_{1-x} with the same P:As ratio used in the starting precursors (within experimental error). In each case the stoichiometry of the ternary precursor was conserved in the product, consistent with an ionic route.

This can be contrasted to ignition synthesis of the analogous Ga(P, As) materials where the stoichiometry of the solid-solution precursor is not conserved.[24b] Reactions between GaI_3 and $Na_3P_xAs_{1-x}$ lead to products which enrich in phosphorus relative to the precursor composition over a range of values of x, from $x = 0.25$ to $x = 0.75$. We suggest that these reactions proceed through elemental intermediates and that the selective enrichment of phosphorus is due

to the fact that phosphorus has a higher vapor pressure than arsenic at the reaction temperature achieved.

In an analogous manner to the (P,As) systems, there is experimental evidence for both routes in the (S,Se) reactions using $Na_2S_xSe_{1-x}$. Reactions between this solid-solution precursor and $CaCl_2$ result in Ca(S,Se) products with conserved stoichiometry, while reactions with $MoCl_5$ yield $Mo(S,Se)_2$ products which are enriched in the more volatile element (sulfur).[25]

It is likely that the stability of a metal ion in the presence of strongly reducing species is important in determining which route will be taken. Based on electrochemical studies of ions in a 450°C KCl-LiCl melt,[37] the reduction potentials of Gd^{3+} ($E_{Gd(III)/Gd(0)}$ = − 2.788 V vs. Pt) and Ca^{2+} ($E°_{Ca(II)/Ca(0)}$ = −3.3 V vs. Pt) are considerably larger than those of Ga^{3+} ($E°_{Ga(III)/Ga(0)}$ = −1.136 V vs. Pt) and Mo^{3+}($E°_{Mo(III)/Mo(0)}$ = −0.603 V vs. Pt). Therefore, Ga^{3+} is more likely to be reduced by the nonmetal anions P^{3-} or S^{2-} in a molten salt rather than Gd^{3+} or Ca^{2+}. For the elemental route, once redox has taken both ions to their zero valent state, there is subsequent reaction between the elements with the heat provided by salt formation. In this case the ternary product becomes enriched in the nonmetal with the higher vapor pressure, relative to the composition of the precursor. In the ionic pathway, a simple metathetical reaction occurs in the byproduct salt flux and no enrichment is observed.

CONCLUSIONS

Rapid solid-state metathesis reactions provide a new synthetic approach to a wide variety of materials. The initiation processes are fairly straightforward: the self-sustaining reactions initiate when at least one of the precursors changes phase by melting, vaporizing, or decomposing. The rapid, exothermic nature of these precursor reactions makes it very difficult to observe directly intermediate species or mechanistic steps, though it is likely that shortly after reaction ignition, under the extreme conditions present, there may be a variety of species present in the reaction flux (ions, elements, molecular fragments, etc.). The fact that these highly reactive species are well-dispersed throughout a high-temperature salt flux accounts for the success of this approach. The diffusion barriers typically

associated with solid–solid reactions are significantly smaller because the particle sizes of the reactants have been reduced to essentially atomic dimensions, allowing for rapid product formation. Even the formation of the salt byproduct seems to promote continued reaction by (a) generating a large amount of heat, and (b) becoming a molten host allowing further reactant diffusion and nucleation of the primary product. The reaction ends when the heat has dissipated and the melt solidifies.

Understanding exactly what happens in the reaction flux is necessary for complete control of this reaction route. The details of the SSM process are currently under investigation, but even without that knowledge, many advantages of this method are already apparent. (1) The solid-state precursor reactions are easily initiated, rapid, and self-sustaining. This reduces the time and energy put into the reaction process. (2) The species within the flux are extremely reactive and finely dispersed. This enables reactions between refractory materials at temperatures far below their bulk melting points. (3) The maximum temperature achieved by the reaction flux and the amount of time at that temperature affects the yield and crystallinity of the products. Larger reaction mixtures are better insulated and lead to greater product crystallinity and yield, whereas adding an inert heat sink to a reaction mixture leads to decreased product crystallinity by lowering the overall temperature. (4) It is possible to form some high-temperature phases through these reactions, such as cubic/tetragonal ZrO_2 and β-$MoSi_2$. (5) The ability to use homogeneous, ternary precursors allows for the synthesis of compositionally uniform mixed-metal and mixed-nonmetal solid-solution materials.

Acknowledgments

The authors gratefully acknowledge Dr. P. R. Bonneau and Dr. J. B. Wiley for fruitful discussions of this research. This work was supported by the National Science Foundation, a Packard Foundation Fellowship, a Sloan Foundation Fellowship, and a Dreyfus Teacher Scholar Award.

References

1. N. B. Pilling and R. E. Bedworth, J. Inst. Metals **1**, 529 (1923).

2. (a) A. Stein, S. W. Keller and T. A. Mallouk, Science **259**, 1558 (1993). (b) R. Roy, Solid State Ionics **32**, 3 (1989).
3. A. G. Merzhanov and I. P. Borovinskaya, Dokl. Akad. Nauk SSSR (Engl. transl.) **204**, 429 (1972).
4. (a) R. W. Cahn, Adv. Mater. **2**, 314 (1990). (b) H. C. Yi and J.J. Moore, J. Mater. Sci. **25**, 1159 (1990). (c) Z. A. Munir and U. Anselmi-Tamburini, Mat. Sci. Reports **3**, 277 (1989).
5. A. Wold, J. Chem. Ed. **57**, 531 (1980).
6. C. J. Brinker and G. W. Scherer, *Sol Gel Science* (Academic Press, Inc., New York, 1990).
7. (a) E. Matijevic, Chem. Mater. **5**, 412 (1993). (b) J. Livage, M. Henry and C. Sanchez, Prog. Sol. St. Chem. **18**, 259 (1988).
8. (a) R. L. Axelbaum, S. E. Bates, W. E. Buhro, C. Frey, K. F. Kelton, S. A. Lawton, L. J. Rosen and S. M. Sastry, Nanostructured Materials **2**, 139 (1992). (b) S. Reich, H. Suhr, K. Hanko and L. Szepes, Adv. Mater. **4**, 650 (1992).
9. (a) R. Fix, R. G. Gordon, and D. M. Hoffman, Chem. Mater. **5**, 614 (1993). (b) T. Wade, R. M. Crooks, E. G. Garza, D. M. Smith, J. O. Willis and J. Y. Coulter, Chem. Mater. **6**, 87 (1994).
10. (a) S. R. Aubuchon, A. T. McPhail, R. L. Wells, J. A. Giambra and J. R. Bowser, Chem. Mater. **6**, 82 (1994).
11. (a) K. Su and L. G. Sneddon, Chem. Mater. **5**, 1659 (1993). (b) K. J. Wynne and R. W. Rice, Ann. Rev. Mater. Sci. **14**, 297 (1984).
12. (a) A Guntz and H. Bassett, Bull. Soc. Chim. (de Paris) **35**(ser. 3), 201 (1906). (b) S. Hilpert and A. Wille, Z. Phys. Chem. **18B**, 291 (1932).
13. J. B. Wiley and R. B. Kaner, Science **255**, 1093 (1992). (b) R. B. Kaner, P. R. Bonneau, E. G. Gillan, J. B. Wiley and R. E. Treece, U. S. Patent 5,110,768 (May 5, 1992).
14. (a) P. R. Bonneau, J. B. Wiley and R. B. Kaner, Inorg. Synth., in press. (b) D. P. Shoemaker, C. W. Garland, J. I. Steinfeld and J. W. Nibler, *Experiments in Physical Chemistry* (McGraw-Hill Book Co., New York, 1981), 4th ed., p. 125.
15. (a) J. C. Fitzmaurice, A. L. Hector and I. P. Parkin, J. Chem. Soc. Dalton Trans. **16**, 2435 (1993). (b) E. G. Gillan and R. B. Kaner, Inorg. Chem., in press.
16. R. E. Treece, G. S. Macala and R. B. Kaner, Inorg. Chem. **4**, 9 (1992).
17. R. E. Treece, G. S. Macala, L. Rao, D. Franke, H. Eckert and R. B. Kaner, Inorg. Chem. **32**, 2745 (1993).
18. (a) L. Rao and R. B. Kaner, Inorg. Chem., **33**, 3210 (1994). (b) R. E. Treece, E. G. Gillan, R. M. Jacubinas, J. B. Wiley and R. B. Kaner, in *Better Ceramics Through Chemistry V*, edited by M. J. Hampden-Smith, W. J. Klemperer and C. J. Brinker (Mat. Res. Soc. Symp. Proc. **271**, Pittsburgh, PA, 1992), p. 169.
19. (a) J. B. Wiley, E. G. Gillan and R. B. Kaner, Mat. Res. Bull. **28**, 893 (1993). (b) A. Hector and I. P. Parkin, Polyhedron **12**, 1855 (1993). (c) A. L. Hector and I. P. Parkin, J. Mat. Sci. Lett. **13**, 219 (1994).
20. (a) A. T. Rowley and I. P. Parkin, J. Mater. Chem. **3**, 689 (1993). (b) R. E. Treece, J. A. Conklin and R. B. Kaner, Inorg. Chem., in press.
21. (a) R. F. Jarvis, Jr., Ph.D. Dissertation, University of California, Los Angeles, 1992. (b) J. C. Fitzmaurice, A. Hector and I. P. Parkin, J. Mat. Sci. Lett. **13** (1994).
22. (a) P. R. Bonneau, R. F. Jarvis, Jr. and R. B. Kaner, Nature **349**, 510 (1991). (b) P. R. Bonneau, R. K. Shibao and R. B. Kaner, Inorg. Chem. **29**, 2511 (1990). (c) I. P. Parkin and A. T. Rowley, Polyhedron **12**, 2961 (1993).
23. R. M. Jacubinas and R. B. Kaner, in *High Temperature Silicides and Refractory Alloys*, edited by C. L. Briant, J. J. Petrovic, B. P. Bewlay, A. K. Vasudevan and H. A. Lipsitt (Mat. Res. Soc. Symp. Proc. **322**, Pittsburgh, PA, 1994).

24. (a) P. R. Bonneau and R. B. Kaner, Inorg. Chem. **32**, 6084 (1993). (b) R. E. Treece, Ph.D. Dissertation, University of California, 1992.
25. P. R. Bonneau, R. F. Jarvis, Jr. and R. B. Kaner, Inorg. Chem. **31**, 2127 (1992).
26. K. A. Schwetz and A. Lipp, in *Ulmann's Encyclopedia of Industrial Chemistry*, edited by W. Gerharz and Y. S. Yamamoto (VCH, Weinheim, FRG, 1985), 5th ed., vol. A4, p. 295.
27. (a) W. Lengauer and P. Ettmayer, Monat. Chem. **117**, 275 (1986). (b) G. Brauer and R. Esselborn, Z. Anorg. Allgem. Chem. **309**, 151 (1961).
28. *CRC Handbook of Chemistry and Physics*, edited by R. C. Weast (CRC Press, Boca Raton, FL, 1993), 74th ed. (b) *Dictionary of Inorganic Compounds*, edited by J. E. Macintyre, F. M. Daniel and V. M. Stirling (Chapman and Hall, New York, 1992), vol. 3.
29. (a) O. Kubaschewski and C. B. Alcock, *Metallurgical Thermochemistry* (Pergamon Press, Inc., New York, 1979), 5th ed. (b) *JANAF Thermochemical Tables*, edited by D. R. Lide, Jr. (ACS and AIP Inc., New York, 1985), 3rd ed.
30. A. Wells, *Structural Inorganic Chemistry* (Clarendon Press, Oxford, 1990), 5th ed, p. 168.
31. (a) R. Nötzel and K. H. Ploog, Adv. Mater. **5**, 22 (1993). (b) C. R. M. Grovenor, *Microelectronic Materials* (Adam Hilger, Philadelphia, PA, 1989).
32. (a) R. W. Siegel, Ann. Rev. Mater. Sci. **21**, 559 (1991). (b) G. E. Fougere, J. R. Weertman, R. W. Siegel and S. Kim, Scripta Metall. et Mater. **26**, 1879 (1992).
33. H. J. Scheel and D. Elwell, *Crystal Growth from High Temperature Solution* (Academic Press, New York, 1975).
34. (a) R. Stevens, *Zirconia and Zirconia Ceramics* (Magnesium Elektron, Ltd. **113**, 1986), 2nd ed. (b) A. H. Heuer, J. Am. Ceram. Soc. **70**, 689 (1987). (c) R. C. Garvie and S.-K. Chan, Physica B **150**, 203 (1988).
35. (a) R. Srinivasan, C. R. Hubbard, O. B. Cavin and B. H. Davis, Chem. Mater. **5**, 27 (1993). (b) V. S. Nagarajan and K. J. Rao, J. Mater. Res. **6**, 2688 (1991). (c) B. E. Yoldas, J. Am. Ceram. Soc. **65**, 387 (1982). (d) A. Chatterjee, S. K. Pradhan, A. Datta, M. De and D. Chakravorty, J. Mater. Res. **9**, 263 (1994).
36. J. J. Petrovic, Mat. Res. Soc. Bull. **18**, 35 (1993).
37. J. A. Plambeck, in *Encyclopedia of Electrochemistry of the Elements*, edited by A. J. Bard (Marcel Dekker, Inc., New York, 1976), vol. 10, pp. 11–84.